

# Dependence of nucleon properties on pseudoscalar meson masses

Amand Faessler<sup>1</sup>, Thomas Gutsche<sup>1</sup>, Valery E Lyubovitskij<sup>1†</sup>,  
Chalump Oonariya<sup>1,2</sup>

<sup>1</sup> Institut für Theoretische Physik, Universität Tübingen,  
Auf der Morgenstelle 14, D-72076 Tübingen, Germany

<sup>2</sup> School of Physics, Suranaree University of Technology,  
111 University Avenue, Nakhon Ratchasima 30000, Thailand

E-mail: amand.faessler@uni-tuebingen.de,  
thomas.gutsche@uni-tuebingen.de,  
valeri.lyubovitskij@uni-tuebingen.de,  
chalump@tphys.physik.uni-tuebingen.de

**Abstract.** We discuss the sensitivity of nucleon properties (mass, magnetic moments and electromagnetic form factors) on the variation of the pseudoscalar meson masses in the context of the perturbative chiral quark model. The obtained results are compared to data and other theoretical predictions.

*PACS:* 12.39.Ki, 12.39.Fe, 13.40.Em, 13.40.Gp, 14.20.Dh

*Keywords:* Nucleon mass, magnetic moments, form factors, meson cloud

† On leave of absence from the Department of Physics, Tomsk State University, 634050 Tomsk, Russia

## 1. INTRODUCTION

In recent years nucleon properties have been in the focus of manifestly Lorentz covariant Chiral Perturbation Theory (ChPT), improved lattice QCD computations and chiral extrapolations (see e.g. Refs. [1]-[23]). The lattice formulation of QCD is well established and is a powerful tool for studying the structure of nucleons. The computation of nucleon properties in lattice QCD is progressing with steadily increasing accuracy [4]-[8]. Accurate computations of the nucleon mass with dynamical fermions and two active flavors are now possible [9, 10] in lattice QCD. In practice, these computations are so far limited to relatively large quark masses. Direct simulations of QCD for light current quark masses, near the chiral limit, remain computationally intensive. To extract predictions for observables, lattice data generated at high current quark masses have to be extrapolated to the point of physical quark or pion mass. Therefore, one of the current aims in lattice QCD is to establish the quark mass dependence of quantities of physical interest, such as the nucleon mass, magnetic moments and form factors. The major tool in establishing the current quark mass dependence of lattice QCD results are methods based on chiral effective field theory. Recent extrapolation studies of lattice results concern the nucleon mass [4, 5, 11, 12, 14], its axial vector coupling constant and magnetic moments [11]-[13], the pion-nucleon sigma term, charge radii [15], form factors [16]-[18], and moments of structure functions [19]. The chiral expansion in chiral effective field theory ( $\chi$ EFT) has been used to study the quark mass (pion mass) dependence of the magnetic moments, magnetic form factors and the axial-vector coupling constant [20, 21] of the nucleon for extrapolations of lattice QCD results, so far determined at relatively large quark masses corresponding to pion masses of  $m_\pi \geq 0.6$  GeV, down to physical values of  $m_\pi$ . In the chiral limit, with  $m_\pi \rightarrow 0$ , QCD at low energies is realized in the form of an effective field theory with spontaneously broken chiral symmetry, with massless pions as the primary active degrees of freedom. The coupling of the chiral Goldstone bosons to these spin-1/2 matter field produces the so-called "pion-cloud" of the nucleon, an important component of nucleon structure at low energy and low momentum scales.

In the present paper we investigate the dependence of nucleon properties (mass, magnetic moments and electromagnetic form factors) on pseudoscalar meson masses applying the perturbative chiral quark model (PCQM) [24]-[26]. In the PCQM baryons are described by three relativistic valence quarks confined in a static potential, which are supplemented by a cloud of pseudoscalar Goldstone bosons, as required by chiral symmetry. This simple phenomenological model has already been successfully applied to the charge and magnetic form factors of baryons, sigma terms, ground state masses of baryons, the electromagnetic  $N \rightarrow \Delta$  transition, and other baryon properties [24]-[26]. Note that in Refs. [27, 28] we extend this approach by constructing a framework which is manifestly Lorentz covariant and aims for consistency with ChPT.

In this work, our strategy is as follows. First, we discuss the nucleon properties (mass, magnetic moments and electromagnetic form factors) in dependence on the

pion mass in the two-flavor sector. Second, we extend our formalism to the three-flavor sector including kaon and  $\eta$ -meson degrees of freedom with fixed masses. All calculations are performed at one loop. The chiral limit, where current quark masses approach zero with  $\hat{m}, m_s \rightarrow 0$ , is well defined. We compare the obtained quark mass dependence of the nucleon observables to the results of other approaches (lattice QCD, chiral extrapolations).

The paper is organized as follows. In Sec. II we give a short overview of our approach. In Sec. III we discuss dependence of nucleon properties on the variation of the pion mass in the two- and three-flavor picture in the context of the PCQM and compare them to other theoretical approaches. In Sec. IV we give our conclusions.

## 2. THE PERTURBATIVE CHIRAL QUARK MODEL

The perturbative chiral quark model [24]-[26] is based on an effective chiral Lagrangian describing baryons by a core of three valence quarks, moving in a central Dirac field with  $V_{\text{eff}}(r) = S(r) + \gamma^0 V(r)$ , where  $r = |\vec{x}|$ . In order to respect chiral symmetry, a cloud of Goldstone bosons ( $\pi$ ,  $K$  and  $\eta$ ) is included, which are treated as small fluctuations around the three-quark core. The model Lagrangian is

$$\begin{aligned} \mathcal{L}(x) = & \bar{\psi}(x) [i \not{\partial} - \gamma^0 V(r) - \mathcal{M}] \psi(x) \\ & + \frac{F^2}{4} \text{Tr} \left[ \partial^\mu U(x) \partial^\mu U^\dagger(x) + 2\mathcal{M}B(U(x) + U^\dagger(x)) \right] \\ & - \bar{\psi}(x) S(r) \left[ \frac{U(x) + U^\dagger(x)}{2} + \gamma^5 \frac{U(x) - U^\dagger(x)}{2} \right] \psi(x), \end{aligned} \quad (1)$$

where  $\psi = (u, d, s)$  is the triplet of quark fields,  $U = \exp[i\hat{\Phi}/F]$  is the chiral field in the exponential parametrization,  $F = 88$  MeV is the pion decay constant in the chiral limit [29],  $\mathcal{M} = \text{diag}\{m_u, m_d, m_s\}$  is the mass matrix of current quarks and  $B = -\langle 0|\bar{u}u|0\rangle/F^2 = -\langle 0|\bar{d}d|0\rangle/F^2$  is the quark condensate constant. In the numerical calculations we restrict to the isospin symmetry limit  $m_u = m_d = \hat{m}$ . We rely on the standard picture of chiral symmetry breaking [30] and for the masses of pseudoscalar mesons we use the leading term in their chiral expansion (i.e. linear in the current quark mass). By construction, our effective chiral Lagrangian is consistent with the known low-energy theorems (Gell-Mann-Okubo and Gell-Mann-Oakes-Renner relations, partial conservation of axial current (PCAC), Feynman-Hellmann relation between pion-nucleon  $\sigma$ -term and the derivative of the nucleon mass, etc.). The electromagnetic field is included into the effective Lagrangian (1) using the standard procedure, i.e. the interaction of quarks and charged mesons with photons is introduced using minimal substitution.

To derive the properties of baryons, which are modeled as bound states of valence quarks surrounded by a meson cloud, we formulate perturbation theory and restrict the quark states to the ground-state contribution with  $\psi(x) = b_0 u_0(\vec{x}) \exp(-i\mathcal{E}_0 t)$ , where  $b_0$  is the corresponding single-quark annihilation operator. The quark wave function  $u_0(\vec{x})$  belongs to the basis of potential eigenstates used for expanding the quark field operator

$\psi(\vec{x})$ . In our calculation of matrix elements, we project quark diagrams on the respective baryon states. The baryon states are conventionally set up by the product of the SU(6) spin-flavor and SU(3)<sub>c</sub> color wave functions, where the nonrelativistic single quark spin wave function is simply replaced by the relativistic solution  $u_0(\vec{x})$  of the Dirac equation

$$\left[ -i\gamma^0 \vec{\gamma} \cdot \vec{\nabla} + \gamma^0 S(r) + V(r) - \mathcal{E}_0 \right] u_0(\vec{x}) = 0, \quad (2)$$

where  $\mathcal{E}_0$  is the single-quark ground-state energy.

For the description of baryon properties, we use the effective potential  $V_{\text{eff}}(r)$  with a quadratic radial dependence [24, 25]:

$$S(r) = M_1 + c_1 r^2, \quad V(r) = M_2 + c_2 r^2 \quad (3)$$

with the particular choice

$$M_1 = \frac{1 - 3\rho^2}{2\rho R}, \quad M_2 = \mathcal{E}_0 - \frac{1 + 3\rho^2}{2\rho R}, \quad c_1 \equiv c_2 = \frac{\rho}{2R^3}. \quad (4)$$

Here,  $R$  and  $\rho$  are parameters related to the ground-state quark wave function  $u_0$ :

$$u_0(\vec{x}; i) = N_0 \exp\left[-\frac{\vec{x}^2}{2R^2}\right] \begin{pmatrix} 1 \\ i\rho \vec{\sigma}(i) \cdot \vec{x}/R \end{pmatrix} \chi_s(i) \chi_f(i) \chi_c(i), \quad (5)$$

where  $N_0 = [\pi^{3/2} R^3 (1 + 3\rho^2/2)]^{-1/2}$  is a normalization constant;  $\chi_s$ ,  $\chi_f$ ,  $\chi_c$  are the spin, flavor and color quark wave functions, respectively. The index "i" stands for the  $i$ -th quark. The constant part of the scalar potential  $M_1$  can be interpreted as the constituent mass of the quark, which is simply the displacement of the current quark mass due to the potential  $S(r)$ . The parameter  $\rho$  is related to the axial charge  $g_A$  of the nucleon calculated in zeroth-order (or 3q-core) approximation:

$$g_A = \frac{5}{3} \left( 1 - \frac{2\rho^2}{1 + \frac{3}{2}\rho^2} \right). \quad (6)$$

Therefore,  $\rho$  can be replaced by  $g_A$  using the matching condition (6). The parameter  $R$  is related to the charge radius of the proton in the zeroth-order approximation as

$$\langle r_E^2 \rangle_{\text{LO}}^P = \int d^3x u_0^\dagger(\vec{x}) \vec{x}^2 u_0(\vec{x}) = \frac{3R^2}{2} \frac{1 + \frac{5}{2}\rho^2}{1 + \frac{3}{2}\rho^2}. \quad (7)$$

In our calculations we use the value  $g_A=1.25$ . Therefore, we have only one free parameter in our model, that is  $R$  or  $\langle r_E^2 \rangle_{\text{LO}}^P$ . In previous publications  $R$  was varied in the region from 0.55 fm to 0.65 fm, which corresponds to a change of  $\langle r_E^2 \rangle_{\text{LO}}^P$  from 0.5 to 0.7 fm<sup>2</sup>. Note that for the given form of the effective potential (3) the Dirac equation (2) can be solved analytically [for the ground state see Eq.(5), for excited states see Ref. [26]].

The expectation value of an operator  $\hat{A}$  is then set up as:

$$\langle \hat{A} \rangle = {}^B \langle \phi_0 | \sum_{n=1}^{\infty} \frac{i^n}{n!} \int d^4x_1 \dots \int d^4x_n T[\mathcal{L}_I(x_1) \dots \mathcal{L}_I(x_n) \hat{A}] | \phi_0 \rangle_c^B, \quad (8)$$

where the state vector  $|\phi_0\rangle$  corresponds to the unperturbed three-quark state (3q-core). Superscript "B" in the equation indicates that the matrix elements have to be projected onto the respective baryon states, whereas subscript "c" refers to contributions

from connected graphs only. Here  $\mathcal{L}_I(x)$  is the appropriate interaction Lagrangian. For the purpose of the present paper, we include in  $\mathcal{L}_I(x)$  the linearized coupling of pseudoscalar fields with quarks and the corresponding coupling of quarks and mesons to the electromagnetic field (see details in Ref. [24]):

$$\begin{aligned} \mathcal{L}_I(x) = & -\bar{\psi}(x)i\gamma^5\frac{\hat{\Phi}(x)}{F}S(r)\psi(x) - eA_\mu(x)\bar{\psi}(x)\gamma^\mu Q\psi(x) \\ & - eA_\mu(x)\sum_{i,j=1}^8\left[f_{3ij} + \frac{f_{8ij}}{\sqrt{3}}\right]\Phi_i(x)\partial^\mu\Phi_j(x) + \dots, \end{aligned} \quad (9)$$

where  $f_{ijk}$  are the SU(3) antisymmetric structure constants.

For the evaluation of Eq. (8) we apply Wick's theorem with the appropriate propagators for the quarks and pions. For the quark propagator we use the vacuum Feynman propagator for a fermion in a binding potential restricted to the ground-state quark wave function with

$$iG_0(x, y) = u_0(\vec{x})\bar{u}_0(\vec{y})e^{-i\mathcal{E}_0(x_0-y_0)}\theta(x_0 - y_0). \quad (10)$$

For the meson field we use the free Feynman propagator for a boson field with

$$i\Delta_{ij}(x - y) = \langle 0|T\{\Phi_i(x)\Phi_j(y)\}|0\rangle = \delta_{ij}\int\frac{d^4k}{(2\pi)^4i}e^{-ik(x-y)}\Delta_\Phi(k), \quad (11)$$

where  $\Delta_\Phi(k) = [M_\Phi^2 - k^2 - i0^+]^{-1}$  is the meson propagator in momentum space and  $M_\Phi$  is the meson mass.

The physical nucleon mass at one loop is given by

$$m_N = m_N^{core} + \Delta m_N \quad (12)$$

where

$$m_N^{core} = 3\left\{\mathcal{E}_0 + \gamma\hat{m}\right\} = 3\left\{\mathcal{E}_0 + \frac{\gamma}{2B}M_\pi^2\right\} \quad (13)$$

is the contribution of the three-quark core (the second term in the r.h.s. of Eq. (13) is the contribution of the current quark mass) and

$$\Delta m_N = \Pi^{MC} + \Pi^{ME} \quad (14)$$

is the nucleon mass shift due to the meson cloud contribution. The diagrams that contribute to the nucleon mass shift  $\Delta m_N$  at one loop are shown in Fig.1 (see details in Refs. [24, 25]). Fig.1a corresponds to the so-called meson-cloud (MC) contribution and Fig.1b is the meson-exchange (ME) contribution. The operators  $\Pi^{MC}$  and  $\Pi^{ME}$  are functions of the meson masses and are expressed in terms of the universal self-energy operator

$$\Pi(M_\Phi^2) = -I_\Phi^{24}, \quad \Phi = \pi, K, \eta. \quad (15)$$

Here we introduce a notation for the structure integral in terms of which all further formulas can be expressed:

$$I_\Phi^{MN} = \left(\frac{g_A}{\pi F}\right)^2 \int_0^\infty \frac{dp p^N F_{\pi NN}^2(p^2)}{(M_\Phi^2 + p^2)^{\frac{M}{2}}}, \quad M, N = 0, 1, 2, \dots \quad (16)$$

and

$$\begin{aligned} I_{\Phi}^{0N} \equiv I_N \equiv & \left(\frac{g_A}{\pi F}\right)^2 \int_0^{\infty} dp p^N F_{\pi NN}^2(p^2) = \left(\frac{g_A}{\pi F}\right)^2 \left(\frac{2}{R^2}\right)^{\frac{N+1}{2}} \\ & \times \Gamma\left(\frac{N+1}{2}\right) \left(\frac{1}{2} - \frac{N+1}{4}\beta + \frac{(N+1)(N+3)}{32}\beta^2\right), \end{aligned} \quad (17)$$

where  $\beta = 2\rho^2/(2-\rho^2)$ . The function  $F_{\pi NN}(p^2)$  is the  $\pi NN$  form factor normalized to unity at zero recoil ( $p^2 = 0$ ):

$$F_{\pi NN}(Q^2) = \exp\left(-\frac{Q^2 R^2}{4}\right) \left\{1 - \frac{Q^2 R^2}{4}\beta\right\}. \quad (18)$$

The meson cloud contributions to the mass shift are then given

1) in SU(2) as

$$\begin{aligned} \Pi^{\text{MC}} &= \frac{81}{400} \Pi(M_{\pi}^2), \\ \Pi^{\text{ME}} &= \frac{90}{400} \Pi(M_{\pi}^2), \end{aligned} \quad (19)$$

2) in SU(3) as

$$\begin{aligned} \Pi^{\text{MC}} &= \frac{81}{400} \Pi(M_{\pi}^2) + \frac{54}{400} \Pi(M_K^2) + \frac{9}{400} \Pi(M_{\eta}^2), \\ \Pi^{\text{ME}} &= \frac{90}{400} \Pi(M_{\pi}^2) - \frac{6}{400} \Pi(M_{\eta}^2). \end{aligned} \quad (20)$$

Exact expressions for the nucleon electromagnetic form factors can be found in Ref. [24]. Here we just present the typical results for the magnetic moments in SU(2) and SU(3). The two-flavor result is obtained from the three-flavor one when neglecting kaon and  $\eta$ -meson contributions. The magnetic moments of the nucleons,  $\mu_p$  and  $\mu_n$ , are given by the expressions

$$\begin{aligned} \mu_p &= \mu_p^{\text{LO}} \left[1 + \delta - \frac{1}{400} \left\{26I_{\pi}^{34} + 16I_K^{34} + 4I_{\eta}^{34}\right\}\right] + \frac{m_N}{50} \left\{11I_{\pi}^{44} + I_K^{44}\right\}, \\ \mu_n &= -\frac{2}{3}\mu_p^{\text{LO}} \left[1 + \delta - \frac{1}{400} \left\{21I_{\pi}^{34} + 21I_K^{34} + 4I_{\eta}^{34}\right\}\right] - \frac{m_N}{50} \left\{11I_{\pi}^{44} + I_K^{44}\right\}, \end{aligned} \quad (21)$$

where

$$\mu_p^{\text{LO}} = \frac{2m_N \rho R}{1 + \frac{3}{2}\rho^2} \quad (22)$$

is the leading-order contribution to the proton magnetic moment. The factor

$$\delta = -\left(\hat{m} + \frac{\Pi^{\text{MC}}}{3} \cdot \frac{1 + \frac{3}{2}\rho^2}{1 - \frac{3}{2}\rho^2}\right) \frac{2 - \frac{3}{2}\rho^2}{\left(1 + \frac{3}{2}\rho^2\right)^2} R \rho \quad (23)$$

defines the NLO correction to the nucleon magnetic moments due to the modification of the quark wave function [24]).

### 3. NUMERICAL RESULTS

In this section we discuss the numerical results for the dependence of nucleon properties on a variation of the pseudoscalar meson masses.

In Table 1 we present our results for the nucleon mass in dependence on the pion mass. Both the SU(2) version, considering only the pion cloud contribution, and the SU(3) variant, including in addition kaon and  $\eta$ -meson cloud contributions, are indicated. The total result is normalized to the physical value (coinciding with the proton mass treated as the reference point)  $m_N \equiv m_p = 938.27$  MeV by fixing the ground-state quark energy to  $\mathcal{E}_0 \simeq 397$  MeV [in case of SU(2)] and  $\mathcal{E}_0 \simeq 411$  MeV [in case of SU(3)]. We also indicate the separate contributions of the 3q-core and the meson cloud, and, in addition, the value obtained in the chiral limit, consistent with the values of Refs. [27, 31, 14]. For the dependence on the pion mass we choose mass values in the range of  $M_\pi^2 \simeq 0.15 - 1.2$  GeV<sup>2</sup> and the resulting nucleon mass is directly compared to either chiral extrapolations or lattice data [7, 8]. In both comparisons our results are consistent with the corresponding values of either the extrapolations or the lattice data. In Figs. 3 and 4 we indicate the full functional dependence of the nucleon mass on  $M_\pi^2$ ,  $M_K^2$  and  $M_\eta^2$ , respectively, and compare them (in case of the SU(2)  $M_\pi^2$ -dependence) to results of lattice QCD at order  $p^3$  and  $p^4$  of Ref.[4]. In Fig. 5 we compare the results for the nucleon mass both in SU(2) and SU(3) to lattice QCD data from various collaborations [7, 8] as functions of  $M_\pi^2$ .

In Table 2 we present our results for the nucleon magnetic moments in the SU(2) version for different values of the model scale parameter  $R$  at  $M_\pi = 0$  and at the physical pion mass  $M_\pi^{\text{phys}}$ . In Table 3 we give the analogous results for SU(3). In Figs. 6 and 7 we draw the curves for the nucleon magnetic moments as functions of  $M_\pi^2$  and compare them to results of lattice QCD [13, 18]. Note, that the nucleon magnetic moments are not sensitive to a variation of the strange current quark mass  $m_s$ . In Figs. 8 and 9 we demonstrate the sensitivity of the nucleon magnetic moments as functions of  $M_\pi^2$  on the variation of the scale parameter  $R$ .

Finally, in Figs. 10-12 we present results for the nucleon form factors  $G_E^p(Q^2)$ ,  $G_M^p(Q^2)/\mu_p$  and  $G_M^n(Q^2)/\mu_n$  at different values of  $M_\pi^2$ . A larger pion mass leads to an increase of the normalized (at  $Q^2 = 0$ ) form factors.

### 4. CONCLUSIONS

In this work we apply the perturbative chiral quark model at one loop to describe the dependence of nucleon properties on the meson masses. It has been previously verified that the model is successful in the explanation of many aspects of nucleon properties [23-25], such as magnetic moments, the axial vector form factor, the  $N \rightarrow \Delta$  transition amplitude, the meson-nucleon sigma-term and  $\pi N$  nucleon scattering. Here we demonstrate that the meson mass dependence of nucleon properties such as the mass, magnetic moments, electromagnetic form factors, both for the two and three flavor

variants, is reasonably described in comparison to present lattice data and extrapolations of these results. Given also the simplicity of this model approach, the evaluation at one loop seems sufficient to correctly describe the pion mass dependence of the discussed observables.

## Acknowledgments

This work was supported by the DFG under contracts FA67/31-1 and GRK683. This research is also part of the EU Integrated Infrastructure Initiative Hadronphysics project under contract number RII3-CT-2004-506078 and President grant of Russia "Scientific Schools" No. 5103.2006.2. The stay in Tübingen of Chalump Oonariya was supported by the DAAD under PKZ:A/05/57631.

- [1] T. Becher and H. Leutwyler, Eur. Phys. J. C **9** (1999) 643 [arXiv:hep-ph/9901384]; JHEP **0106** (2001) 017 [arXiv:hep-ph/0103263]; P. J. Ellis and H. B. Tang, Phys. Rev. C **57** (1998) 3356 [arXiv:hep-ph/9709354]; B. Kubis and U. G. Meissner, Nucl. Phys. A **679** (2001) 698 [arXiv:hep-ph/0007056]; Eur. Phys. J. C **18** (2001) 747 [arXiv:hep-ph/0010283]; M. R. Schindler, J. Gegelia and S. Scherer, Phys. Lett. B **586** (2004) 258 [arXiv:hep-ph/0309005]; Eur. Phys. J. A **19** (2004) 35 [arXiv:hep-ph/0309234]; M. R. Schindler, J. Gegelia and S. Scherer, Eur. Phys. J. A **26** (2005) 1 [arXiv:nucl-th/0509005]; B. C. Lehnhart, J. Gegelia and S. Scherer, J. Phys. G **31** (2005) 89 [arXiv:hep-ph/0412092]; M. R. Schindler, D. Djukanovic, J. Gegelia and S. Scherer, Phys. Lett. B **649** (2007) 390 [arXiv:hep-ph/0612164]; M. R. Schindler, T. Fuchs, J. Gegelia and S. Scherer, Phys. Rev. C **75** (2007) 025202 [arXiv:nucl-th/0611083]; V. Bernard, Prog. Part. Nucl. Phys. **60** (2008) 82 [arXiv:0706.0312 [hep-ph]].
- [2] D. B. Leinweber, D. H. Lu and A. W. Thomas, Phys. Rev. D **60** (1999) 034014 [arXiv:hep-lat/9810005].
- [3] D. B. Leinweber, A. W. Thomas and R. D. Young, Phys. Rev. Lett. **92** (2004) 242002 [arXiv:hep-lat/0302020].
- [4] M. Procura, B. U. Musch, T. Wollenweber, T. R. Hemmert and W. Weise, Phys. Rev. D **73** (2006) 114510 [arXiv:hep-lat/0603001].
- [5] M. Procura, T. R. Hemmert and W. Weise, Phys. Rev. D **69** (2004) 034505 [arXiv:hep-lat/0309020].
- [6] M. Procura, B. U. Musch, T. R. Hemmert and W. Weise, Phys. Rev. D **75** (2007) 014503 [arXiv:hep-lat/0610105].
- [7] B. Orth, T. Lippert and K. Schilling, Phys. Rev. D **72** (2005) 014503 [arXiv:hep-lat/0503016].
- [8] A. Ali Khan *et al.* [QCDSF-UKQCD Collaboration], Nucl. Phys. B **689** (2004) 175 [arXiv:hep-lat/0312030].
- [9] A. Ali Khan *et al.* [CP-PACS Collaboration], Phys. Rev. D **65** (2002) 054505 [Erratum-ibid. D **67** (2003) 059901] [arXiv:hep-lat/0105015].
- [10] S. Aoki *et al.* [JLQCD Collaboration], Phys. Rev. D **68** (2003) 054502 [arXiv:hep-lat/0212039].
- [11] R. D. Young, D. B. Leinweber and A. W. Thomas, Prog. Part. Nucl. Phys. **50** (2003) 399 [arXiv:hep-lat/0212031].
- [12] V. Bernard, T. R. Hemmert and U. G. Meissner, Nucl. Phys. A **732** (2004) 149 [arXiv:hep-ph/0307115].
- [13] B. R. Holstein, V. Pascalutsa and M. Vanderhaeghen, Phys. Rev. D **72** (2005) 094014 [arXiv:hep-ph/0507016].
- [14] M. Frink, U. G. Meissner and I. Scheller, Eur. Phys. J. A **24** (2005) 395 [arXiv:hep-lat/0501024].

- [15] E. J. Hackett-Jones, D. B. Leinweber and A. W. Thomas, Phys. Lett. B **494** (2000) 89 [arXiv:hep-lat/0008018].
- [16] T. R. Hemmert and W. Weise, Eur. Phys. J. A **15** (2002) 487 [arXiv:hep-lat/0204005]; T. R. Hemmert, M. Procura and W. Weise, Phys. Rev. D **68** (2003) 075009 [arXiv:hep-lat/0303002].
- [17] D. B. Leinweber, A. W. Thomas, K. Tsushima and S. V. Wright, Phys. Rev. D **61** (2000) 074502 [arXiv:hep-lat/9906027].
- [18] P. Wang, D. B. Leinweber, A. W. Thomas and R. D. Young, Phys. Rev. D **75** (2007) 073012 [arXiv:hep-ph/0701082].
- [19] W. Detmold, W. Melnitchouk, J. W. Negele, D. B. Renner and A. W. Thomas, Phys. Rev. Lett. **87** (2001) 172001 [arXiv:hep-lat/0103006].
- [20] T. R. Hemmert, M. Procura and W. Weise, Phys. Rev. D **68** (2003) 075009 [arXiv:hep-lat/0303002].
- [21] M. Procura, B. U. Musch, T. R. Hemmert and W. Weise, AIP Conf. Proc. **842** (2006) 240.
- [22] E. J. Hackett-Jones, D. B. Leinweber and A. W. Thomas, Phys. Lett. B **489** (2000) 143 [arXiv:hep-lat/0004006].
- [23] T. R. Hemmert, M. Procura and W. Weise, Nucl. Phys. A **721** (2003) 938 [arXiv:hep-lat/0301021].
- [24] V. E. Lyubovitskij, T. Gutsche and A. Faessler, Phys. Rev. C **64** (2001) 065203 [arXiv:hep-ph/0105043].
- [25] V. E. Lyubovitskij, T. Gutsche, A. Faessler and E. G. Drukarev, Phys. Rev. D **63** (2001) 054026 [arXiv:hep-ph/0009341]; V. E. Lyubovitskij, T. Gutsche, A. Faessler and R. Vinh Mau, Phys. Lett. B **520** (2001) 204 [arXiv:hep-ph/0108134]; Phys. Rev. C **65** (2002) 025202 [arXiv:hep-ph/0109213]; V. E. Lyubovitskij, P. Wang, T. Gutsche and A. Faessler, Phys. Rev. C **66** (2002) 055204 [arXiv:hep-ph/0207225]; F. Simkovic, V. E. Lyubovitskij, T. Gutsche, A. Faessler and S. Kovalenko, Phys. Lett. B **544** (2002) 121 [arXiv:hep-ph/0112277].
- [26] S. Cheedket, V. E. Lyubovitskij, T. Gutsche, A. Faessler, K. Pumsa-ard and Y. Yan, Eur. Phys. J. A **20** (2004) 317 [arXiv:hep-ph/0212347]; K. Pumsa-ard, V. E. Lyubovitskij, T. Gutsche, A. Faessler and S. Cheedket, Phys. Rev. C **68** (2003) 015205 [arXiv:hep-ph/0304033]; T. Inoue, V. E. Lyubovitskij, T. Gutsche and A. Faessler, Phys. Rev. C **69** (2004) 035207 [arXiv:hep-ph/0311275]; K. Khosonthongkee, V. E. Lyubovitskij, T. Gutsche, A. Faessler, K. Pumsa-ard, S. Cheedket and Y. Yan, J. Phys. G **30** (2004) 793 [arXiv:hep-ph/0403119].
- [27] A. Faessler, T. Gutsche, V. E. Lyubovitskij and K. Pumsa-ard, Phys. Rev. D **73** (2006) 114021 [arXiv:hep-ph/0511319].
- [28] A. Faessler, T. Gutsche, B. R. Holstein, V. E. Lyubovitskij, D. Nicmorus and K. Pumsa-ard, Phys. Rev. D **74** (2006) 074010 [arXiv:hep-ph/0608015]; A. Faessler, T. Gutsche, V. E. Lyubovitskij and K. Pumsa-Ard, Prog. Part. Nucl. Phys. **55** (2005) 12; A. Faessler, T. Gutsche, V. E. Lyubovitskij and K. Pumsa-Ard, AIP Conf. Proc. **884** (2007) 43; A. Faessler, T. Gutsche, B. R. Holstein, V. E. Lyubovitskij, D. Nicmorus and K. Pumsa-ard, arXiv:hep-ph/0612246; A. Faessler, T. Gutsche, B. R. Holstein, V. E. Lyubovitskij, in preparation.
- [29] J. Gasser, M. E. Sainio and A. Svarc, Nucl. Phys. B **307** (1988) 779.
- [30] J. Gasser and H. Leutwyler, Phys. Rept. **87** (1982) 77; Nucl. Phys. B **250** (1985) 465.
- [31] B. Borasoy and U. G. Meissner, Annals Phys. **254** (1997) 192 [arXiv:hep-ph/9607432].

**Table 1.** Nucleon mass (in GeV) in the SU(2) and SU(3) versions and at different values for  $M_\pi^2$

Nucleon mass	SU(2)	SU(3)	Other approaches
3q-core	1.203	1.247	-
Meson loops (total)	-0.265	-0.309	-
$\pi$ loops	-0.265	-0.265	-
$K$ loops	-	-0.042	-
$\eta$ loops	-	-0.002	-
Total	0.93827	0.93827	-
Chiral limit	0.887	0.831	0.880 [5, 12]; 0.883 [4]; 0.770(110) [31]; 0.890(180) [14]; 0.832 [27]
$M_\pi^2$ (in GeV $^2$ )			
0.153	1.122	1.128	1.182(26) [7]
0.162	1.133	1.138	1.195(42) [7]
0.175	1.148	1.154	1.104(20) [7]
0.240	1.212	1.220	1.228(31) [7]
0.348	1.310	1.320	1.356(21) [7]
0.413	1.360	1.371	1.377(19) [7]
0.462	1.400	1.412	1.410(17) [7]
0.557	1.475	1.490	1.533(28) [7]
0.588	1.500	1.515	1.509(16) [7]
0.678	1.566	1.582	1.637(27) [7]
0.774	1.638	1.656	1.631(30) [7]
0.810	1.664	1.682	1.619(16) [7]
0.258	1.231	1.239	1.253(15) [8]
0.271	1.240	1.248	1.275(82) [8]
0.297	1.266	1.275	1.300(22) [8]
0.310	1.275	1.284	1.320(19) [8]
0.314	1.280	1.288	1.412(61) [8]
0.354	1.314	1.324	1.348(13) [8]
0.502	1.431	1.444	1.497(77) [8]
0.514	1.442	1.456	1.506(94) [8]
0.536	1.458	1.742	1.509(18) [8]
0.540	1.462	1.476	1.519(11) [8]
0.578	1.493	1.507	1.657(26) [8]
0.607	1.515	1.530	1.629(20) [8]
0.776	1.640	1.658	1.679(36) [8]
0.874	1.710	1.730	1.741(29) [8]
0.883	1.717	1.736	1.781(15) [8]
0.894	1.725	1.744	1.878(28) [8]
0.901	1.730	1.749	1.785(35) [8]
0.913	1.738	1.758	1.798(85) [8]
0.921	1.744	1.764	1.801(14) [8]
0.940	1.758	1.778	1.809(17) [8]
1.201	1.943	1.965	2.063(26) [8]

**Table 2.** Nucleon magnetic moments in SU(2)

R (fm)	$\mu_p$		$\mu_n$	
	$M_\pi = 0$	$M_\pi^{\text{phys}}$	$M_\pi = 0$	$M_\pi^{\text{phys}}$
0.50	3.896	2.984	-2.948	-2.015
0.55	3.828	2.947	-2.871	-1.970
0.60	3.796	2.945	-2.823	-1.952
0.65	3.792	2.969	-2.797	-1.954
0.70	3.803	3.012	-2.789	-1.973

**Table 3.** Nucleon magnetic moments in SU(3) for fixed masses  $M_K^2$  and  $M_\eta^2$ 

R (fm)	$\mu_p$		$\mu_n$	
	$M_\pi = 0$	$M_\pi^{\text{phys}}$	$M_\pi = 0$	$M_\pi^{\text{phys}}$
0.50	3.512	2.598	-2.976	-2.043
0.55	3.466	2.585	-2.984	-1.993
0.60	3.456	2.605	-2.843	-1.972
0.65	3.471	2.648	-2.815	-1.972
0.70	3.505	2.709	-2.804	-1.988

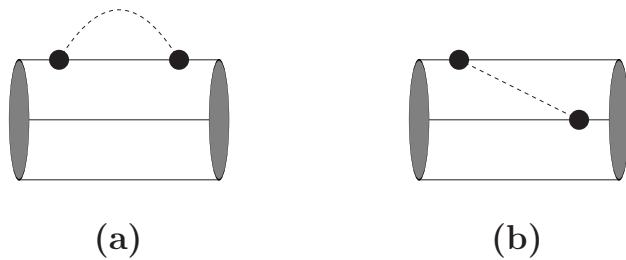


**Figure 1.** Diagrams contributing to the nucleon mass shift.

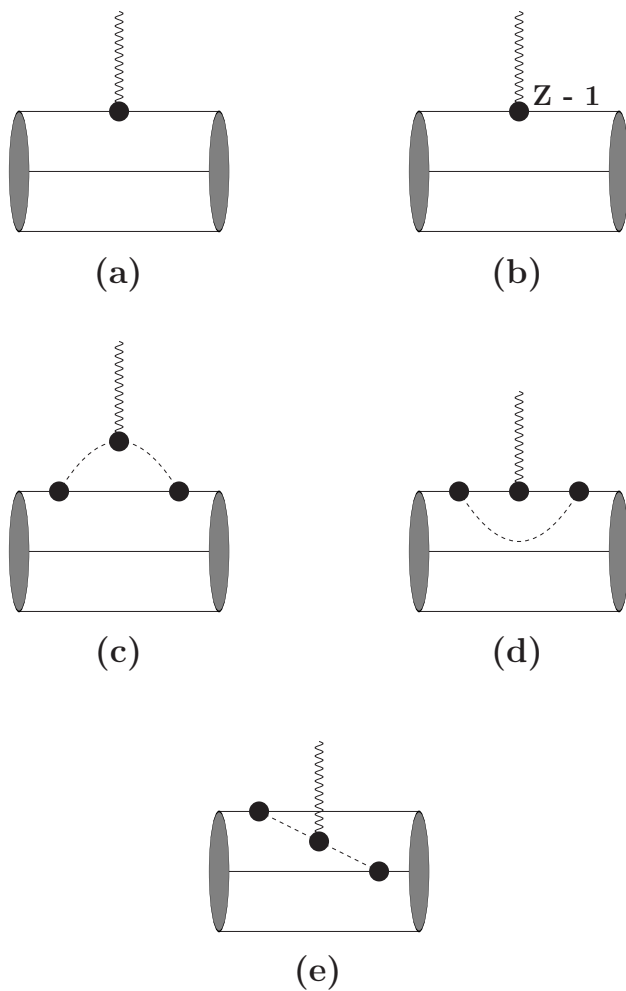


**Figure 2.** Diagrams contributing to the nucleon electromagnetic form factors.

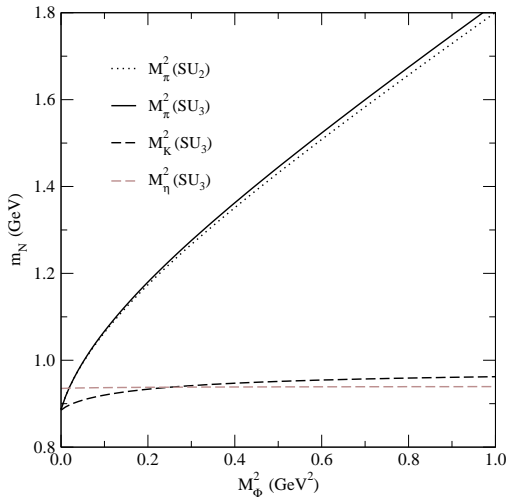


**Figure 3.** Dependence of nucleon mass  $m_N$  on meson mass  $M_\Phi^2$ :  $m_N(M_\pi^2)$  in SU(2) (dotted line) and  $m_N(M_\pi^2)$ ,  $m_N(M_K^2)$ ,  $m_N(M_\eta^2)$  in SU(3) (the other lines).

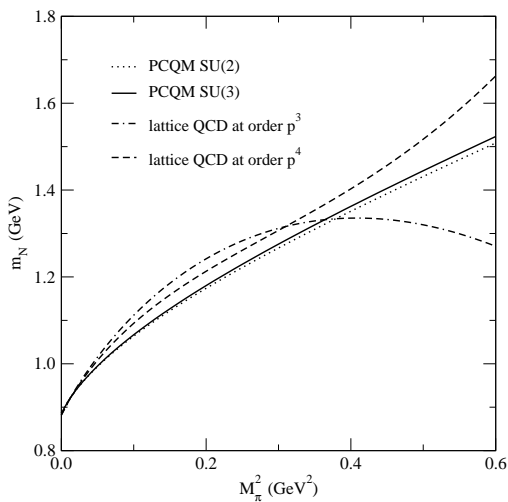


**Figure 4.** Dependence of nucleon mass  $m_N$  on pion mass  $M_\pi^2$ :  $m_N(M_\pi^2)$  in SU(2) (dotted line), SU(3) (solid line) and from lattice QCD [4] (the others) at order  $p^3$  and  $p^4$ .

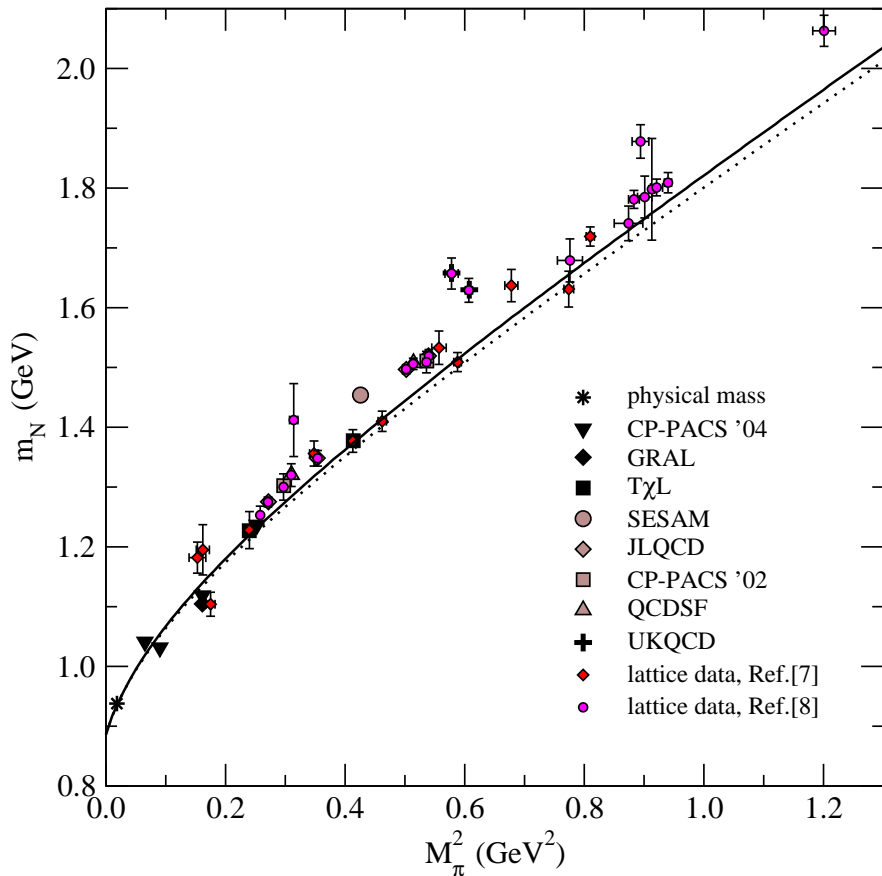


**Figure 5.** Nucleon dependencies  $m_N(M_\pi^2)$  in  $SU(2)$  (dotted line) and in  $SU(3)$  (solid line) are compared to data from various collaborations as a function of  $M_\pi^2$ .

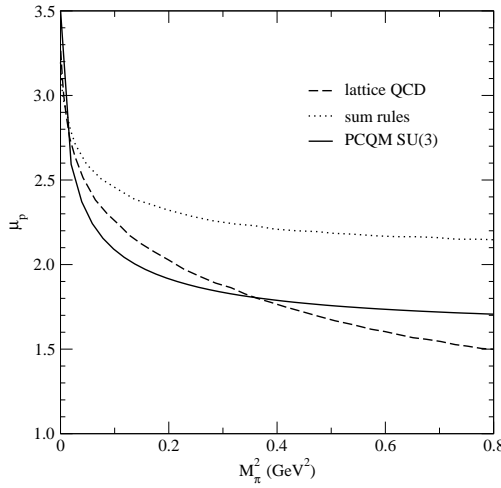


**Figure 6.**  $M_\pi^2$ -dependence of the proton magnetic moment  $\mu_p(M_\pi^2)$  to one-loop from sum rules [13] (dotted curve), lattice QCD [18] (dashed curve) and our results in SU(3) (solid curve).

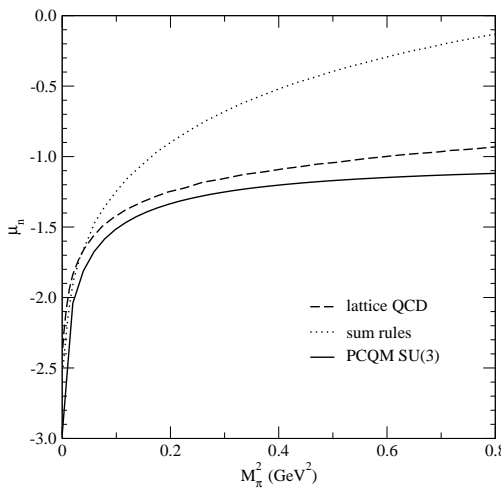


**Figure 7.**  $M_\pi^2$ -dependence of the neutron magnetic moment  $\mu_n(M_\pi^2)$  to one-loop from sum rules [13] (dotted curve), lattice QCD [18] (dashed curve) and our results in SU(3) (solid curve).

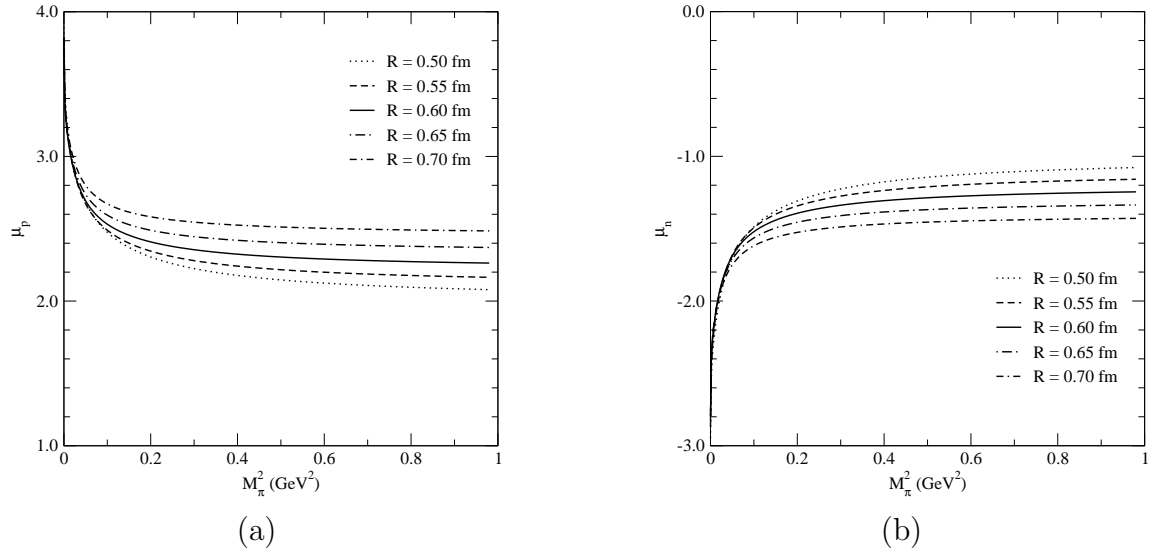


**Figure 8.**  $\mu_N$  at  $M_\pi^2 = 0 - 1 \text{ GeV}^2$  and  $R = 0.5 - 0.7 \text{ fm}$  in SU(2).

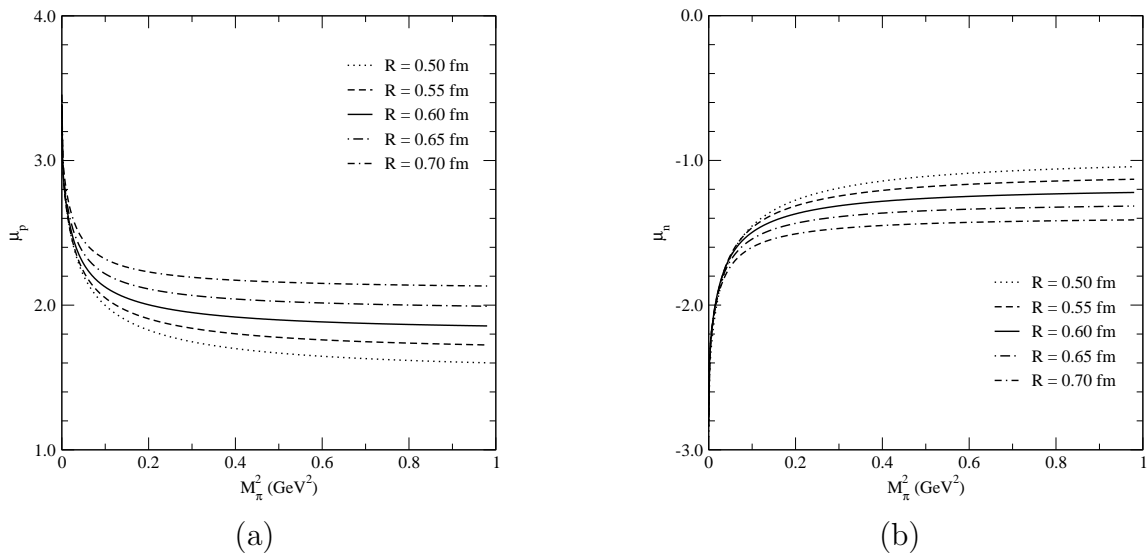


**Figure 9.**  $\mu_N$  at  $M_\pi^2 = 0 - 1$  GeV $^2$  and  $R = 0.5 - 0.7$  fm in SU(3).

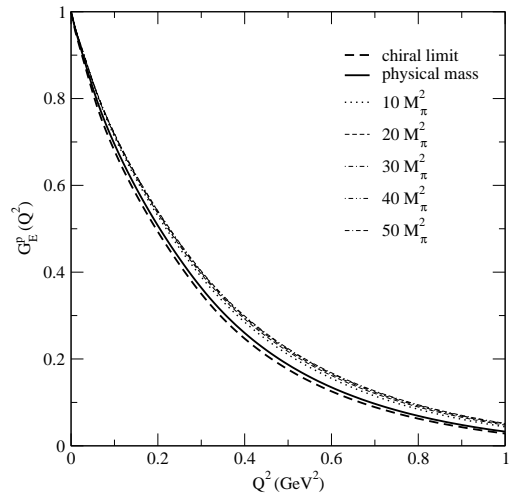


**Figure 10.** Proton charge form factor  $G_E^p(Q^2)$  as function of  $M_\pi^2$  in SU(2).

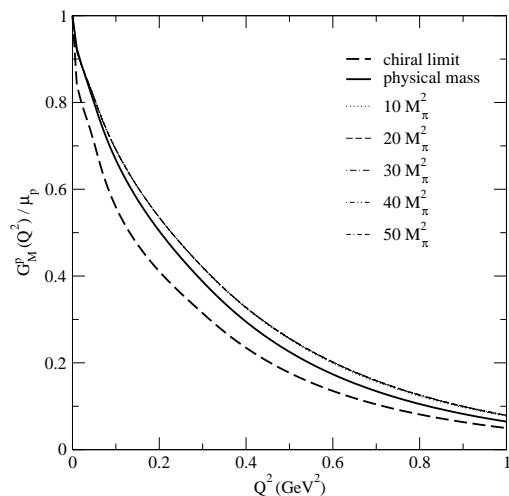


**Figure 11.** Proton magnetic form factor  $G_M^p(Q^2)$  as function of  $M_\pi^2$  in SU(2).

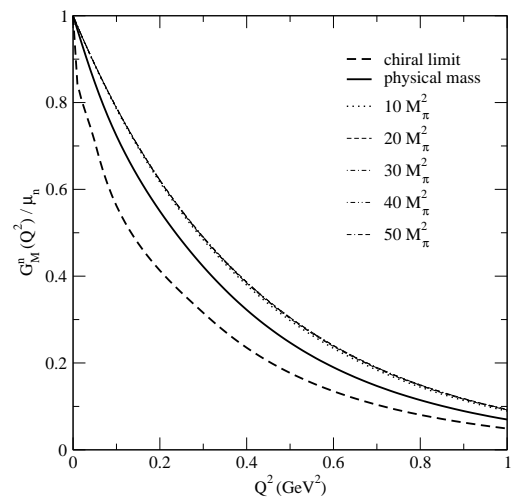


**Figure 12.** Neutron magnetic form factor  $G_M^n(Q^2)$  as function of  $M_\pi^2$  in SU(2).